LUMINESCENCE FROM VACUUM-ULTRAVIOLET–IRRADIATED COSMIC ICE ANALOGS AND RESIDUES

MURTHY S. GUDIPATI,[1,2,3] JASON P. DWORKIN,[2,4] XAVIER D. F. CHILLIER,[5] AND LOUIS J. ALLAMANDOLA[2]

ABSTRACT

Here we report a study of the optical luminescent properties for a variety of vacuum-ultraviolet (VUV)–irradiated cosmic ice analogs and the complex organic residues produced. Detailed results are presented for the irradiated, mixed molecular ice: $H_2O : CH_3OH : NH_3 : CO$ (100 : 50 : 1 : 1), a realistic representation for an interstellar/precometary ice that reproduces all the salient infrared spectral features associated with interstellar ices. The irradiated ices and the room-temperature residues resulting from this energetic processing have remarkable photoluminescent properties in the visible (520–570 nm). The luminescence dependence on temperature, thermal cycling, and VUV exposure is described. It is suggested that this type of luminescent behavior might be applicable to solar system and interstellar observations and processes for various astronomical objects with an ice heritage. Some examples include grain temperature determination and vaporization rates, nebula radiation balance, albedo values, color analysis, and biomarker identification.

Subject headings: astrochemistry — dust, extinction — ISM: molecules — methods: laboratory — molecular data

1. INTRODUCTION

Mixed molecular ices are common to planets, their satellites, and comets in the solar system and probably other planetary systems as well (e.g., Cruikshank 1997; Schmitt, deBergh, & Festou 1998; Cruikshank 1999; Roush 2001 and references therein), and they are a major component of the dust in dense molecular clouds (e.g., Ehrenfreund & Charnley 2000; Gibb et al. 2000). Laboratory studies of interstellar and precometary ice analogs have shown that cosmic-ray and vacuum-ultraviolet (VUV) processing produces nonvolatile organics with a wide range of chemical complexity (e.g., Bernstein et al. 1995; Greenberg et al. 2000; Cottin, Szopa, & Moore 2001b; Dworkin et al. 2001; Gerakines, Moore, & Hudson 2001; Hudson & Moore 2001; Moore, Hudson, & Gerakines 2001; Kobayashi et al. 2001; Strazzulla & Palumbo 2001; Bernstein et al. 2002; Muñoz Caro et al. 2002). The dark objects in the outer solar system and the organic crust on comets as well as the dust in their comae are likely to be rich in these materials. Similar irradiation studies of planetary ice analogs have come to similar conclusions (McDonald 1996; Cruikshank 1997; Schmitt, deBergh, & Festou 1998; Cruikshank 1999; Roush 2001).

Apart from contributing to the chemical inventory and history of these objects, when in sufficient abundance, these chemically complex new materials also contribute to their spectroscopic properties. Over the past 30 years, emphasis has focused on the infrared (IR) properties of these materials. However, in the optical spectral region (ultraviolet [UV], visible, and near-IR) the spectral properties of these products are also important because they can directly affect the albedo and wavelength-dependent reflectivity and, in the case of particles, influence the temperature. Furthermore, in some instances, UV-pumped visible and near-IR luminescence could mislead the interpretation of reflectivity and albedo measurements of objects. Similarly, given the current interest in developing spectroscopic tools to search for signs of previous or current biological activity on other planets, it is important to characterize the luminescent properties of these nonbiogenic organic materials since many biomolecules also have similar optical properties. The optical properties of this prebiotic ingredient should be considered when one is searching for biomarkers to separate false from true spectroscopic biosignatures on planets and other astronomical objects that could potentially harbor life.

There have been only a few studies of the luminescence from astrophysically relevant ice analogs, some from pure water ice bombarded with high-energy particles (e.g., Langford, McKinley, & Quickenden 2000), others formed by plasma deposition of molecular mixtures (e.g., Wdowiak et al. 1989), as well as work on the thermo- and photoluminescence from interstellar ice analogs (van IJzendoorn 1985, pp. 105–114). Here we report a study of the optical luminescent properties of irradiated interstellar/precometary ice analogs and the complex organic residues produced. We show that irradiated realistic ice analogs and the products resulting from energetic processing of these ices have remarkable photoluminescent properties in the visible, which should be considered when one is interpreting the spectra of various astronomical objects with an ice heritage.

2. EXPERIMENTAL TECHNIQUES

The experimental setup used for the optical absorption and emission studies is schematically shown in Figure 1. The ices were formed by flowing premixed gases onto a cold (13 K) MgF_2 window mounted in a high-vacuum chamber.

[1] Institute of Physical Sciences and Technology, University of Maryland, College Park, MD 20742; also associated with Institut für Physikalische Chemie, Universität zu Köln, Luxemburger Strasse 116, 50939 Köln, Germany.

[2] NASA Ames Research Center, Mail Stop 245-6, Moffett Field, CA 94035-1000.

[3] Corresponding author; mgudipati@mail.arc.nasa.gov.

[4] Laboratory for Extraterrestrial Physics, Code 691, NASA Goddard Space Flight Center, Greenbelt, MD 20771.

[5] Département de chimie-physique, Sciences II/Université de Genève, 30 quai E. Ansermet, CH-1211 Geneva 4, Switzerland.
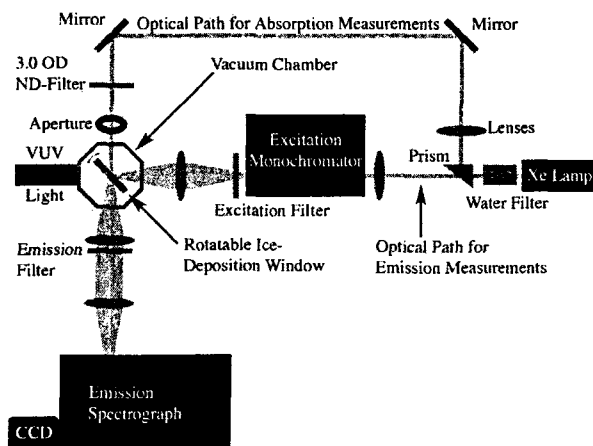
FIG. 1.—Schematic of the optical configuration for emission and absorption studies.

The window was cooled by a closed cycle, helium refrigerator. To maximize photolysis efficiency, the parent gases were deposited for periods of 6–24 hr at ~0.02 mmol hr^{-1} with simultaneous VUV irradiation. Irradiation was carried out with a flowing hydrogen discharge lamp, providing VUV light at Lyα (121.6 nm) as well as a broad range of wavelengths centered around 160 nm due to molecular hydrogen transitions. A detailed description of the cryogenic photolysis system can be found elsewhere (Allamandola, Sandford, & Valero 1988). Deposition protocol was standardized after several attempts resulting in transparent ices. See Dworkin et al. (2001) for a discussion of the reagents and deposition conditions used in this study.

Optical spectra of these ices were recorded at different doses of hydrogen discharge radiation. For absorption studies, as illustrated in Figure 1, the full spectrum from a 150 W Xe arc lamp (Osram/Oriel) was diverted through a prism, collimated through a lens, and finally passed, undis-Q8 persed, through a 3.0 OD neutral density filter and an aperture onto the cold ice films. The transmitted light was then collimated and focused on the entrance slits of a 0.25 m monochromator (Oriel MS 257) equipped with a CCD camera (Oriel-InstaspecIV) to record the spectra. Attempts to measure absorption spectra were unsuccessful mainly because of the scattering of the ices and perhaps because of the inherently broad and structureless absorption features of the irradiated ices. To study the wavelength-dependent emission properties of these ices, light from the same Xe arc lamp was focused onto the entrance slit of a 0.2 m excitation monochromator (Photon Technology International), with which the excitation wavelength could be selected. To avoid light contamination from higher grating orders, appropriate filters were used at the excitation monochromator exit slit before the light was focused onto the ice samples. Optical emission from ices induced by this excitation was then collimated and focused onto the entrance slits of the 0.25 m monochromator, and the emission spectra were recorded with the CCD camera, as described above. A detailed Q9 description of these optical components is provided in Chillier et al. (2002). The irradiance of a 150 W Xe arc lamp is more or less constant at 10 mW m^{-2} nm^{-1} in the range between 310 and 500 nm that is of interest in the present

study. Thus, the ice emission and excitation spectra are not influenced by the lamp profile.

In addition to the filters required to remove the higher order light contamination typical for gratings, both excitation and emission radiation also had to be appropriately and carefully filtered to avoid stray light from the strongly scattering irradiated ices. Without these filters, misleading spectral artifacts would contaminate the spectra. However, after warming to sublimate the unreacted ice, the remaining residue was far less scattering.

Another very important consideration is the excitation-luminescence sampling configuration. This can be used as an additional constraint for those astronomical observations for which it is possible to monitor the phase angle. Observationally, this phenomenon might appear as a reversible shift in broad spectral structure with solar phase angle. The effect is strong enough to significantly alter the spectrum under certain conditions. The two different spectra shown from the same sample in Figure 2 demonstrate the extent to which the broad spectral profile characteristic of luminescence from these complex organic materials can be altered simply by optical configuration. These spectra were measured from nonvolatile organic residue at 300 K using the two different excitation-emission configurations shown schematically in Figure 2. In the reflection configuration (emission collected from the same side of the sample exposed to exciting radiation), the emission at the shorter wavelengths is enhanced with respect to that of the transmission configuration. Conversely, when the emission was collected from the back side of the window-ice/residue sample (transmission configuration) in which the excitation and luminescent light must pass through the sample and window before collection, the emission is enhanced at the longer wavelengths with respect to that measured using the reflection configuration. This phenomenon arises whenever the
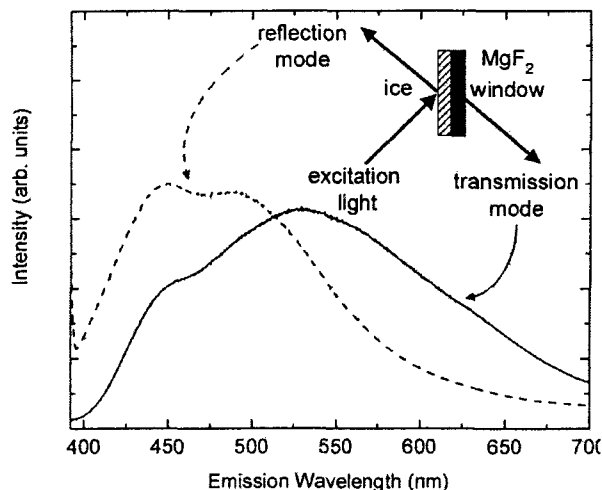

FIG. 2.—Luminescence spectral dependence on excitation-collection optical configuration. Sample: nonvolatile organic residue at 300 K. In the reflection mode, the emission is collected from the same side of the sample that is exposed to the exciting radiation. In the transmission mode, the emission is collected from the backside of the window, after the excitation light and emission light passes through the residue. In both cases the angle between excitation and emission optical paths was kept close to 90° to avoid stray light.

absorption and emission spectra overlap within a sample and is caused by the self-absorption of the shorter wavelength emission by the material when the transmission mode Q10 is used. Here this is due to the broad nature of the absorption and emission features and their overlap between roughly 350 and perhaps 500 nm. As discussed below, continuous, overlapping absorption due to different chromophores results in a broad continuous emission. Whereas the longer wavelength emission passes through the sample, shorter wavelength emission can be absorbed by the longer wavelength absorbing chromophores. The orientation of the sample is reported with each spectrum presented here. We may note that, in principle, this phenomenon can be tested by varying the thickness of the ice films. We expect the emission spectra measured in transmission mode to shift toward the spectra measured in reflection mode as the ice films become thinner.

FIG. 3.—Spatial dependence of the UV-induced (λ_{ex} = 380 nm) emission spectrum from the ice, $H_2O : CH_3OH : NH_3 : CO$ (100 : 50 : 1 : 1), after half of the ice disk was exposed to ionizing radiation. The half-shaded symbol in the upper left represents the ice sample, with the numbered arrows showing the positions for the correspondingly labeled emission spectra. Data were taken in the transmission orientation.

3. LUMINESCENCE FROM IRRADIATED EXTRATERRESTRIAL ICE ANALOGS

This study was undertaken to test whether the complex molecules produced by irradiation of realistic interstellar/precometary ice analogs possessed luminescent or other optical properties that could be used as a diagnostic of the presence of complex organics in astronomical objects with an irradiated ice heritage. To this end, the ices studied here Q11 are related to the parent mixture, which reproduces most of the major IR features of ices in dense molecular clouds along lines of sight toward high-mass protostars, $H_2O : CH_3OH : NH_3 : CO$ (100 : 50 : 1 : 1), ice 1 in Table 1. Upon VUV irradiation of this mixture, all of the major and minor IR bands arising from interstellar ices are reproduced in the spectrum, showing that the composition and concentrations of this mixture are in reasonable agreement with infrared observations (Allamandola et al. 1988; Bernstein et al. 1995). Thus, we refer to this as a realistic interstellar ice Q12 analog.

Prior to investigating these and other ices, we carried out Q13 the following experiment to test that ice irradiation is necessary to observe any emission. One-half of the window on which the ice sample was being deposited was shaded from the VUV photolysis lamp while ice film deposition was kept uniform over the entire cold window. Although some scattered light made it onto the shaded region, one half of the
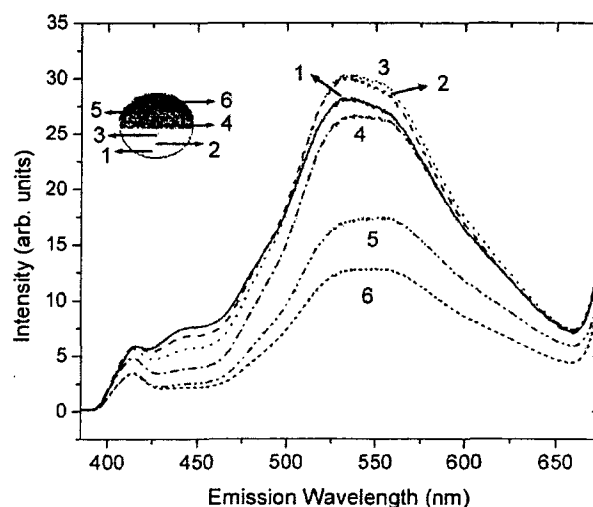
ice film was photolyzed far more than the other half. The emission spectra measured in the transmission orientation from various regions of the ice film stimulated by excitation at 380 nm are shown in Figure 3. These different spectra were measured by sampling the emission from different regions of the ice while keeping all the other parameters fixed. The relative strengths of these spectra as a function of position on the window clearly demonstrate that the shaded (less irradiated) regions of the ice film emit less compared to the fully exposed area, confirming that emission originates in photoproducts. Similar to the solid line in Figure 2, these spectra also show that, when measured in transmission mode, the emission is dominated by a strong, broad, double-humped, structureless band from roughly 460 to 650 nm with maxima near 530 and 550, with several weak shorter wavelength shoulders between 400 and 500 nm.

Different ices were then investigated to constrain the process (Table 1). First, since the CH_3OH concentration is now known to fall between 5% and 30% of the water (Gibb

TABLE 1
SUMMARY OF ICE COMPOSITION AND POST-VUV PHOTOLYSIS LUMINESCENCE BEHAVIOR

		EMISSION MAXIMUM (IN TRANSMISSION MODE) (nm)	
ICE NUMBER	ICE COMPOSITION	Ice	Residue
1	$H_2O : CH_3OH : NH_3 : CO$ (100 : 50 : 1 : 1)	530	510
2	$H_2O : CH_3OH : NH_3 : CO$ (100 : 10 : 1 : 1)	550	530
3	$H_2O : CH_3OH : CO$ (100 : 50 : 1)	530	550
4[a]	$H_2O : CH_3OH : NH_3 : CO : CO_2 : CH_4$ (100 : 4 : 5 : 7.5 : 7.5 : 2)	550	550
5[b]	$H_2O : CO : NH_3 : CH_4$ (5 : 3 : 2 : 1)	520	Not investigated
6	H_2O	None	None

[a] Alternative mixture to simulate dense molecular clouds along lines of sight toward high-mass protostars based on *Infrared Space Observatory* spectra (P. Ehrenfreund 2002, private communication).
[b] van IJzendoorn 1985.

et al. 2000 and references therein), two mixtures with lower than 50% methanol abundance were also studied, ices 2 and 4 in Table 1. In particular, ice 4 (Table 1) was recommended by P. Ehrenfreund (see also Ehrenfreund & Charley 2000) as representative of the then-known best values for an interstellar ice analog. To test whether nitrogen was a critical component of the luminescent chromophores, an interstellar ice analog was studied that did not contain nitrogen in any form (ice 3). Last, pure water ice (ice 6) was irradiated as an additional control. Irradiation of ices 1–5 produces materials with luminescent properties (Table 1) that are very similar to those shown in Figure 3. Given the spectral breadth of the feature and lack of substructure, the various ices considered here, including those devoid of nitrogen, produce luminescent species with similar spectra upon VUV irradiation. Our results are also consistent with earlier work (van IJzendoorn 1985) on photolyzed ices of $H_2O:CO:NH_3:CH_4$ (5:3:2:1). We may note that van IJzendoorn's mixture was studied before IR observations constrained the ice component concentrations. The emission spectrum recorded by van IJzendoorn of VUV-irradiated ices stimulated by 385 nm photon excitation resembles that reported here. It consisted of a very broad band peaking near 520 nm with an FWHM of about 120 nm spanning the range between 410 and 620 nm. It has been shown (Allamandola et al. 1988; Schutte, Allamandola, & Sandford 1993; Bernstein et al. 1995; Dworkin et al. 2001) that variations in the methanol concentration produce the same suite of products but at lower concentrations. It seems likely that the chromophores in the complex organics derived from photolyzed ices containing CH_3OH or CO and CH_4, as in van IJzendoorn's (1985) study, are as similar as their luminescence spectra.

The luminescence observed from a VUV-irradiated ice is very similar to that of the residue remaining after warming (§ 3.3). This shows that the basic organic chromophores in the room-temperature residue are produced immediately upon photolysis in the 10–20 K ice. Warm-up resulting in recombination of smaller radicals is not necessary to produce these organic chromophores. However, warm-up may be necessary to result in cross-linking of these basic chromophores to generate larger molecules without inducing significant changes in the electronic states of the basic chromophore units. The similarities in emission maxima for the ice and the residue spectra listed in Table 1 show that there is no observable change in conjugation upon warm-up. This is remarkable in view of the mass spectral analysis of the room-temperature residual material, which reveals that it is a complex mixture containing hundreds of unsaturated compounds likely containing aromatic, olefinic, and acetylenic chromophores (J. P. Dworkin et al. 2003, in preparation). The in situ, low-temperature production of the essential chromophores of such complex species is consistent with the earlier observation by Schutte et al. (1993) that bands corresponding to the residual materials are already evident in the IR spectra of ices as they are warmed from about 12 to 40 K.

3.1. General Absorption and Emission Properties in the UV–Visible Region

To obtain a general overview of the excitation-emission properties of these samples, three-dimensional excitation and emission spectra were measured covering 280–500 nm

in absorption and 340–700 nm in emission in the reflection orientation. These data are shown over the entire wavelength region studied for the residue at 15 K (Fig. 4). In Figure 4a, the contour plots of spectra measured for shorter excitation and emission wavelengths using a 380 nm cutoff filter for emission are shown, whereas Figure 4b contains the longer wavelength excitation and emission spectra, also shown as contour plots, obtained by using a 510 nm cutoff filter for the emission. When the residue is excited at wavelengths longward of 380 nm, the emission consists of a single maximum near 500 nm, whereas excitation below 380 nm stimulates an additional component near 450 nm. This is illustrated by the two emission spectra shown in Figure 4c, which are taken from the two-dimensional contours in Figure 4a, measured at excitation wavelengths 400 and 360 nm. This observation indicates that the residue consists of several chromophores, whose absorption and emission spectra span a broad wavelength range. Chromophores absorbing at the shorter wavelengths of the broad absorption band also emit in the shorter wavelength region of the broad emission band. It is evident from Figure 4b that absorption of the residue extends into the visible region, up to 475 nm.
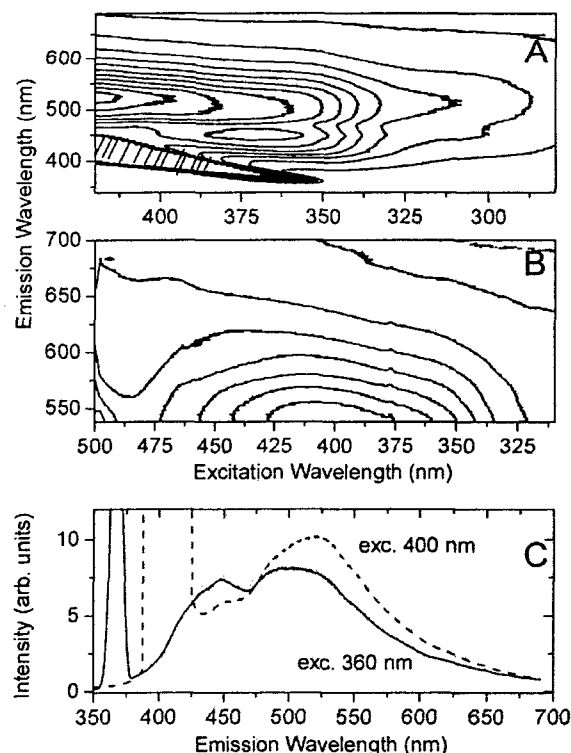

FIG. 4.—Contour plots showing the excitation-emission properties of the complex organic residue at 15 K. This residue was produced by the VUV irradiation of the ice $H_2O:CH_3OH:NH_3:CO$ (100:50:1:1) at 15 K, subsequent warm-up under vacuum to remove the volatile components, and recooling to 15 K. The contour plots show the residue emission properties extending from about 300 nm into the visible region using no excitation filter. (a, b) Luminescence when, respectively, a 380 and 510 nm emission cutoff filter was employed. The shaded artifact is due to the removal of intense stray excitation light. (c) Emission spectra ($\lambda_{ex} = 400$ and 360 nm) extracted from the contour plot in (a). Data were taken in the reflection orientation.

3.2. *Temperature-dependent Emission Spectroscopy of Irradiated Ice*

To understand the changes occurring in the emission spectra as a function of temperature and correlate them to the changes in the morphology as well as phase transitions and phase separation that occur in the ice mixture with changing temperature, we have carried out a careful step-by-step warming of the ices and recorded emission spectra at each of these temperatures. The overall temperature-dependent behavior of the ice luminescence is first presented, followed by a detailed analysis.

Figure 5 shows the temperature dependence of the emission spectrum (transmission orientation) as the sample is first warmed from 13 to 300 K under dynamic vacuum (Fig. 5, *top panel*) and then recooled to 13 K (Fig. 5, *bottom panel*), both in 25 K steps. During this warming the unreacted parent species sublime along with the more volatile photoproducts. These volatile species constitute the major portion of the sample (Bernstein et al. 1995; Dworkin et al 2001). These spectra show a significant decrease of emission intensity in going from 13 to 250 K (Fig. 5, *top panel*). Remarkably, the emission changes in spectral character and regains its intensity as the sample is recooled to 13 K (Fig. 5, *bottom panel*). As it is recooled to 13 K, the non-volatile, residual material becomes more luminescent, with the maximum of the green emission shifting to shorter wavelengths (500–525 nm) compared to the emission from the irradiated ices before sublimation (525–550 nm). The
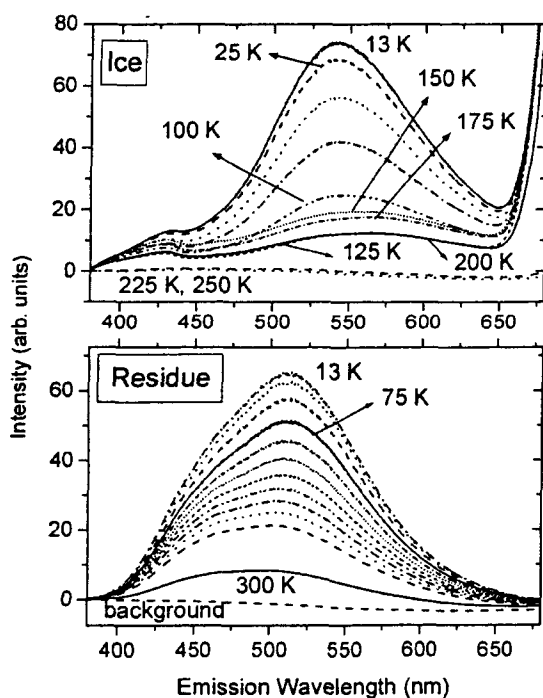

FIG. 6.—Emissivity behavior with temperature and time. (*a*) Filled circles show the emission intensity at 550 nm (λ_{ex} = 360 nm) at a given temperature during warming from 15 to 300 K. At temperatures when time-dependent emission is measured, the points shown correspond to t = 0 data. Filled diamonds show the emission intensity after recooling to 15 K after warming to the given temperature. Open circles give a measure of the time elapsed during the warm-up procedure. The W shape in the emission intensity with temperature curve (*filled circles*) reflects irreversible phase transitions in the ices at the positions indicated with arrows. The minimum at 125 K corresponds to the ice undergoing an amorphous to mixed phase transition, the 145 K maximum to the transformation of H_2O to the hexagonal form (I_h), and the 210 K minimum to the onset of rapid volatile sublimation. (*b*) Monitoring the emission at three temperatures over time. The curves at 125 and 145 K are probably due to the cross-linking of the chromophores and annealing of the ice at that temperature, whereas the 300 K curve is likely due to the loss of luminescence-quenching volatiles, e.g., H_2O. See text for more discussion.

FIG. 5.—UV-induced (λ_{ex} = 380 nm) emission spectra from a photolyzed ice and resulting nonvolatile residue. *Top:* Emission from the ice $H_2O : CH_3OH : NH_3 : CO$ (100 : 50 : 1 : 1) as it is warmed from 25 to 250 K in 25 K steps. *Bottom:* Emission from the nonvolatile residue as it is cooled from 300 to 25 K in 25 K steps. Data were taken in the transmission orientation.
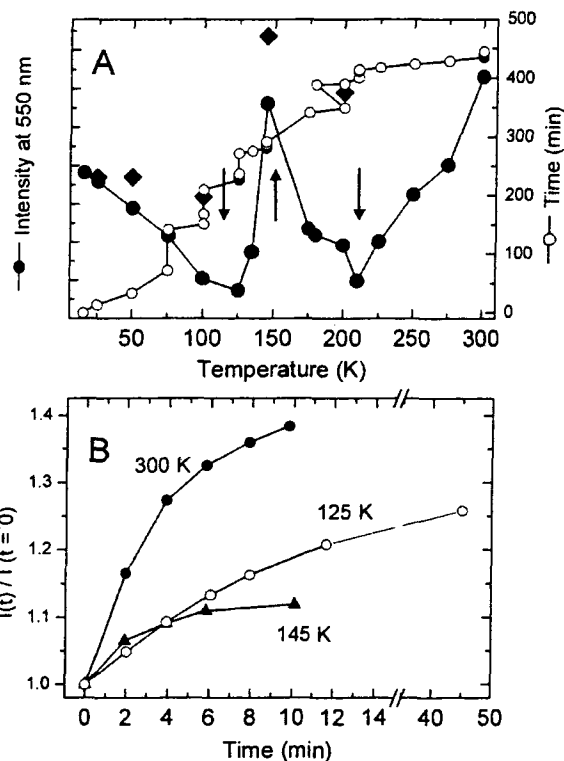
increase in intensity with decreasing temperature suggests that the emission is likely to be due to phosphorescence (Birks 1970). We will come back to the finer details of this behavior later.

The results of a more detailed temperature study are shown in Figure 6. In Figure 6*a* both intensity and time are plotted against temperature. The filled circles and solid line show the emission intensity at 550 nm (λ_{ex} = 360 nm) as the sample was warmed from 15 to 300 K. The sample was recooled to 15 K at several steps during this warm-up, and these 15 K intensities are indicated by the filled diamonds at 25, 50, 100, 145, and 200 K. The open circles present the time history of this warm-up. For example, warming from about 15 to 75 K proceeded smoothly over a period of 60 minutes. The sample was then held at 75 K for roughly 80 minutes.

Several conclusions regarding phase transitions and morphologies can be drawn from this figure. The solid circles

show that there is a steady decrease in the emission intensities from 15 to 125 K. Upon continued warming, there is a sudden jump in emission intensity at 145 K. At this temperature, the transparent ices become translucent. Further temperature increase leads to a precipitous drop in the emission intensity, which then holds steady up to roughly 210 K. Around this temperature the emission intensity starts to rise as the sample is warmed to 300 K. These results indicate that there are three temperatures at which the emission behavior is altered by phase transitions. These are the minimum at 125 K, the sudden jump at 145 K, and the minimum at 210 K. These demarcation temperatures correspond to well-known structural transitions in $H_2O : CH_3OH$ mixed molecular ices. The first minimum at 125 K likely corresponds to crystallization and phase separation similar to that reported by Blake et al. (1991) for $H_2O : CH_3OH$ (2 : 1) at 120 K. In their transmission electron microscope studies, the $H_2O : CH_3OH$ (2 : 1) mixed molecular ice separated into domains of the type II methanol : water clathrate and a grain boundary phase of nearly pure methanol. Similarly, the maximum at 145 K probably corresponds to transformation of H_2O to the hexagonal form (I_h) as also reported by Blake et al. (1991). During this transition, the ices also visually change from a clear transparent film to a translucent powder-like material. As the temperature is further increased, the intensity continues to decrease up to 210 K and then steadily rises. The steady rise from 210 K to room temperature coincides with volatile sublimation, as indicated by increasing pressure in the sample chamber.

Keeping the sample at a given temperature for some time results in an intensity increase (Fig. 6b). The rate of increase in the emission intensity at 550 nm is very similar at 125 and 145 K, suggesting that in this temperature range the cross-linking between the chromophores occurs (along with the phase transitions in the ice itself) at a similar rate. At 300 K this rate is much faster because of the sublimation of the volatiles and formation of the solid nonvolatile residue.

The behavior on thermal cycling back to 15 K as indicated by the filled diamonds supports the conclusion of irreversible phase and structural changes during the first two temperature domains discussed above (15–125 and 125–145 K). As shown by the filled diamonds in Figure 6a, when the sample was recooled to 15 K after reaching 25, 50, and 100 K, emission intensity is largely recovered. Hence, we conclude that the changes that occur (physical or chemical) in these ices between 15 and 100 K are reversible. However, at [Q15] 145 K, an irreversible transition occurs, which is reflected by the sudden large jump in the emission efficiency. As mentioned above, this change at 145 K, which corresponds to the formation of hexagonal water ice (I_h), is accompanied by the visual observation that the ices become translucent. Thus, the architecture of the ice changes, and it may be inferred that the organic and water phases start separating, similar to the process that occurs upon emulsification. Since the emission must originate in the organic species, the emission efficiency should increase. For most organic molecules, luminescence quantum efficiency is higher in organic solvents than in water because water quenches electronic excitations in molecules far more efficiently than organic solvents such as methanol (e.g., Birks 1970). Recooling to 15 K after the precipitous drop between 145 and 175 K and during warming to 210 K results in emission, which is more intense than from the original VUV-irradiated ice (Fig. 6,

filled diamonds at 145 and 200 K). Again, we conclude that the changes are largely reversible. Above 210, the volatiles, including water, leave the sample. Because water is the main quencher of the emission, the emissivity of the ices increases with decreasing water content. We ascribe the steep and steady emission intensity gain between 210 and 300 K to the continued sublimation of water, leaving behind the nonvolatile, complex, organic residue. This nonvolatile residue at 300 K is nearly twice as luminescent as the irradiated ices at 15 K (Fig. 6).

Sample thermal history including ice warm-up rate and how long they are held at a given temperature also influences the emissivities of their residues. For example, the warm-up shown in Figure 5 has been carried out in 25 K steps, the next temperature reached within 5 minutes immediately after recording the spectrum, which took 2 minutes. Thus, the warm-up was complete within about 100 minutes. Because of the fact that the increments were large (25 K), the ice sublimed quickly between 200 and 225 K. We also note that the 300 K residue emission intensity is only about 15% of the 13 K ice emission intensity (as can be seen in Fig. 5). Conversely, at 300 K the residue emission intensity is nearly twice that of the ice at 15 K, when the ice was warmed up more slowly (Fig. 6a).

On the other hand, the general behavior of the temperature dependence of luminescence, with two minima at 125 and 210 K and three maxima at 15, 150, and 300 K (the W-shaped intensity profile) shown in Figure 6a, is also qualitatively seen in the spectra shown in Figure 5. We may note that the spectra were flat at 225 and 250 K but gained intensity at 300 K (Fig. 5, *bottom panel*). A minimum in emissivity was reached at 125 K (Fig. 5, *top panel*), which grew slightly, but significantly, at 150 K, in accordance with the data shown in Figure 6a. However, this growth was not quantitatively comparable with the data shown in Figure 6a, where the sample has been kept at 125 K over 50 minutes. In the former the ice was heated after 7 minutes to the next temperature, 150 K, immediately after taking the spectrum. It is sometimes difficult to separate the effect of time from temperature because they are interdependent in the present case. However, based on the experimental data shown in Figures 5 and 6, we can deduce the following. The changes that occur in the chromophores at 125 K are very significant. The more time spent at this temperature, the more chromophores are retained in the residue, most probably through cross-linking to form less volatile molecules. It is reasonable that the chromophores synthesized by VUV irradiation polymerize through cross-linking and agglomer- [Q16] ate slowly upon warming. If the ices are warmed up quickly, less agglomeration/cross-linking occurs and some of the more volatile chromophores sublime off, while slower warming allows for more of the volatile chromophores to cross-link to form larger nonvolatile molecules. Finally, the emission intensity of the nonvolatile residue increases between 4 and 8 times when cooled from 300 to 15 K. Thus, compared to the irradiated cold ices at 15 K, the nonvolatile [Q17] residues are nearly 1 order of magnitude more luminescent.

We have shown here that time spent by the UV-irradiated ices at a given temperature as well as the temperature gradient strongly influences the efficiency of formation of the nonvolatile residue. Quantitative studies taking these aspects as well as the thermal behavior of a given object of interest with cosmic ices into consideration would help in [Q18] estimating the amount of residue on that object.

3.3. Temperature-dependent Emission Spectroscopy of Nonvolatile Residue

As with the ices, we have also investigated the temperature dependence of the residue emission. Figure 7 shows the UV-pumped luminescent behavior as a function of temperature from two separate residues; the top spectra are of a freshly prepared sample held under vacuum measured in the reflection orientation, while the bottom spectra (measured in the transmission orientation) are of a sample that was prepared 9 months earlier and exposed to the atmosphere during the intervening time then dissolved in chloroform and spotted on the window. Figure 7 shows that there is an overall change in the emission spectrum between these two samples. The UV-pumped emission from the fresh sample (FWHM $\sim$ 170 nm) is double peaked, with two comparably strong, broad components centered near 450 and 500 nm, while the emission from the sample that had been exposed to the atmosphere for nearly 9 months is single peaked, also broad (FWHM $\sim$ 140 nm), and redshifted to 580 nm. Although there may have been changes in the composition of the samples, the underlying chemical properties that account for the general UV-pumped emission of an intense, broad feature spanning most of the visible remains. We also note, as mentioned in the legend to Figure 7, that the spectra from the freshly prepared residue were measured in reflec-

tion mode whereas the spectra of the 9 months old residue were recorded in transmission mode. The spectral shift between part A and part B of Figure 7 arises from a combination of the age of the residue and the mode of observation of the luminescence.

Although the emission spectra are somewhat different, emission from both residues shows the same intensity reversibility with thermal cycling as does the unevaporated ice discussed in the previous section. Figure 7 shows that for both residues, as the temperature is lowered, the emissivity increases with nearly complete reversibility. The protocol for the fresh sample involved first warming the irradiated ice up to room temperature and holding it there for 15 minutes to eliminate the volatile parent and photoproduct molecules. A few small intensity differences are seen in the fresh sample emissivities during thermal cycling, especially between 100 and 250 K. These arise, as indicated by changes in the background pressure of the vacuum chamber, because all of the volatile materials had not yet completely sublimed during the first warm-up. This behavior is different from the nearly perfectly reversible temperature-dependent luminosity of the residue that was shelved at room temperature for about 9 months that is shown in Figure 7 (bottom panel). Based on the close to 1 order of magnitude increase in the emission intensity of the residue going from 300 to 15 K, we propose that the colder an object with a history of ice sublimation, the stronger should be the color in the visible to near-IR region.

3.4. Nonvolatile Residue Emission and VUV Irradiation

The influence of VUV irradiation on the residue's photoluminescent properties was also studied. A freshly irradiated ice was warmed to 300 K and recooled to 15 K. The remaining residue was then irradiated with the hydrogen flow discharge lamp for 300 minutes. The spectra in Figure 8, all taken in reflection orientation, show that low-temperature VUV irradiation does not change the emission spectrum. However, and in sharp contrast to the thermal behavior described above, the emission properties of photolyzed residues are surprising. First, as shown in Figure 8 (left panel), VUV photolysis at 15 K causes a significant loss of emissivity. Second, the decrease in the emissivity observed during warm-up of the photolyzed residue is not 1 order of magnitude as would be expected from an unphotolyzed residue (Fig. 7a). Third, when the irradiated residue was recooled from 300 to 15 K, it regained most of the emission efficiency of the original, unphotolyzed, cold residue (Fig. 8, right panel).

Whether the photolysis-induced changes are physical or chemical in nature is not clear. Figure 8 shows that increasing the temperature from 15 to 300 K apparently reverses Q19 the radiation damage, rending the emitting species back to their initial efficiencies more or less linearly with temperature. This indicates either the reformation of photodestroyed emitting species or the physical rearrangement of the emitting species back to the apparently more efficient, initial configuration.

In either case, the behavior is consistent with the emission expected from a mixture of large functionalized organic molecules. The observation that the spectrum is simply reduced but not altered by VUV irradiation indicates that the emission efficiency of the chromophores responsible for the emission is reduced. Upon VUV irradiation at low tem-
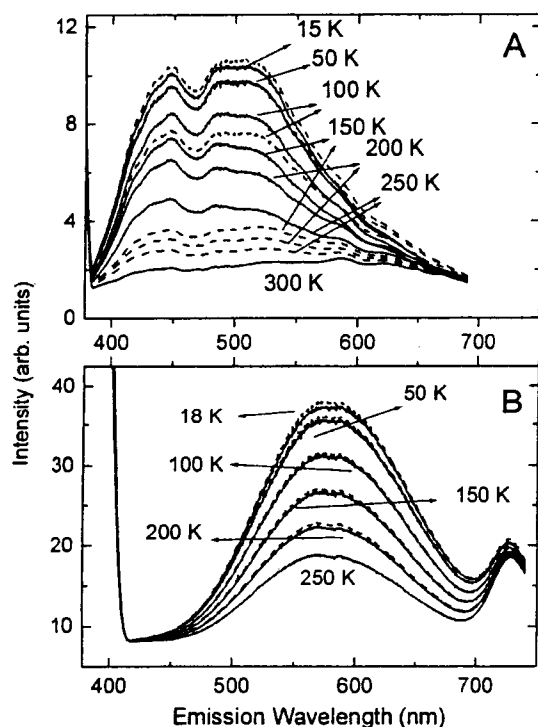
FIG. 7.—Reversibility of residue emission with temperature between 15 and 300 K. The temperature cycle is 15–300–15 K. (a) Emission from a freshly prepared residue. (b) Emission from a residue that has been stored under atmospheric conditions for 9 months. At a given temperature, the emission spectra measured during warm-up are given by solid lines, during cool-down by broken lines. Note that the top spectra were taken in reflection mode and the bottom spectra in transmission mode. The gross spectral shifts between (a) and (b) are due to a combination of the history of the residue and the mode of observation of the luminescence.
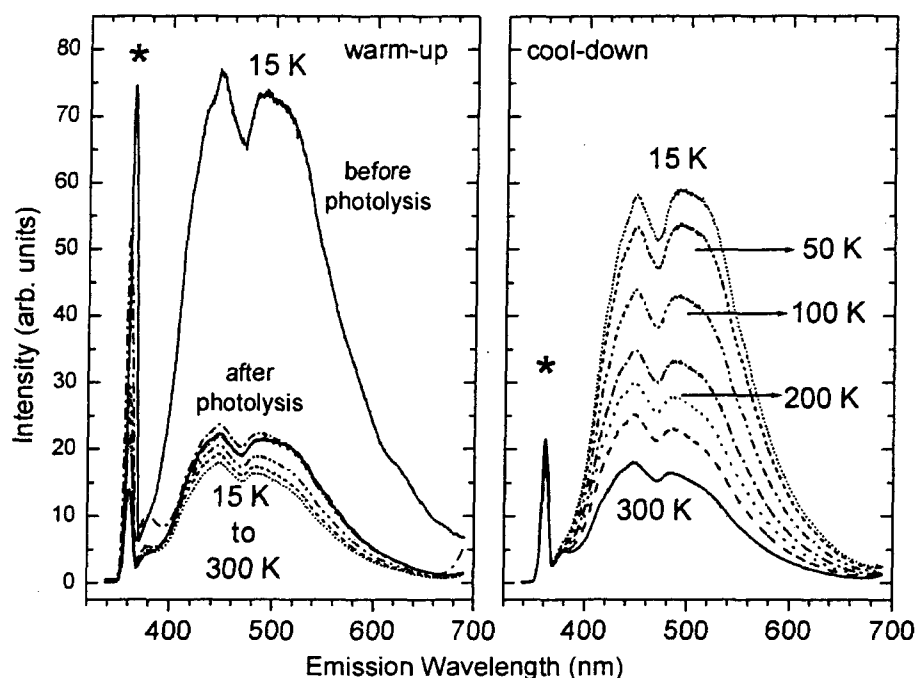
FIG. 8.—Residue emissivity as a function of VUV photolysis and thermal cycling. *Left:* Residue spectrum measured at 15 K before additional VUV photolysis is compared with the spectra measured from the same residue after VUV photolysis at 15 K and during the warm-up to 300 K. *Right:* Spectra of the same residue measured as it was recooled to 15 K. These spectra were measured with the sample in the reflection orientation. Sharp bands marked with asterisks are due to scattered excitation light.

perature either the optimized structure is disturbed similar to amorphization of ices by ultraviolet radiation (Kouchi & Kuroda 1990) or structural and chemical alteration of crystalline olivine under low-energy He$^+$ irradiation (Demyk et al. 2001) or through photolysis the larger molecules are broken into smaller species. Upon warm-up, annealing to the optimum structure or recombination of the fragments reforms the larger, more efficiently emitting molecules.

4. ASTROPHYSICAL APPLICATIONS

There are several different types of astronomical objects, including icy planets and satellites, comets, Kuiper belt objects, reflection nebulae and other dusty interstellar regions, in which blue, UV, and VUV absorption followed by visible and near-IR luminescence can influence observational properties (e.g., albedo and color) as well as radiation balance in the environment. Resolving luminescence from these objects may provide a new spectral and analytical tool, to better understand their surface composition. As illustration of this potential application, two examples of how this process may influence observations and their interpretation will be presented. Furthermore, because many biomolecules also have similar optical properties, these properties should Q20 also be taken into consideration during searches for spectroscopic biosignatures on other planets and satellites. For example, emission spectra of green grasses, when excited at 355 nm, show a prominent blue fluorescence band near 450 nm (A. Schuerger 2002, private communication), close to the strongest component of the emission reported here when measured in the reflection configuration (e.g., Figs. 2, 7a, and 8). Clearly, the chromophores in our residues are differ-

ent from those in grass, so great care should be taken in assessing spectroscopic biosignatures.

Any comparison of the luminescence of the ice and its residue we make in this article is only qualitative. This paper aims at qualitative description of various processes that lead to the observation of luminescence from irradiated ices and Q21 its residue. In order to get a quantitative estimate, more quantitative studies have to be carried out. These will Q22 involve obtaining the concentration of the chromophores, quantum efficiency of the emission with temperature, and lifetime of the luminescence and extinction coefficients, to mention a few. These parameters warrant further laboratory studies.

4.1. Comets

The process of UV-pumped visible luminescence has the potential to influence two distinct areas of comet science. The first has to do with coma grain temperatures and, in turn, extended source distributions. As discussed by Crifo (1987), and extensively by Greenberg & Li (1998), cometary grain temperatures are calculated on the basis of the dust energy balance between grain heating by absorption and cooling by emission. Since radiative cooling is generally assumed to follow the Planck function, most of this cooling radiation falls in the IR and is determined by IR emissivities. However, in addition to this, the UV-pumped luminescent process described here provides another channel through which this absorbed energy can be released. Since this short-lived luminescence releases some of the absorbed energy orders of magnitude more quickly than the IR emission, the equilibrium grain temperatures will be cooler than predicted by models based solely on an emission spectrum

determined by the Planck function. For large grains, the quantum efficiency for this process is likely on the order of 10%, a value typical for bulk organic materials (e.g., Smith & Witt 2002), but as the particles become smaller and smaller at greater distances from the nucleus because of evaporation and degradation, the quantum efficiency will approach the molecular limit, which is typically between 90% and 100% for luminescent molecules (e.g., Birks 1970). Thus, grain temperature behavior as a function of nuclear distance can be quite complex, but in all cases equilibrium temperatures are likely to be cooler than currently calculated, with temperatures per unit mass dropping with grain age and size, behavior that is just the opposite of that expected from a Planck blackbody-controlled thermal dependence where smaller grains would get significantly warmer. This different temperature behavior can significantly affect the rate at which volatiles contained in the grains in the coma evaporate, thereby influencing the extended source coma replenishment rates. Apart from simple photoproducts such as CO trapped in the grains treated by Greenberg & Li (1998), Cottin et al. (2001a) have modeled polyoxymethylene grains as a possible extended source of formaldehyde and daughter molecules such as CO, CO_2, HCOOH, CH_3OH, etc., which have all been detected in comet P/Halley. Here, too, the extended source grain temperature behavior can be significantly different from that assumed. The importance of this process can be modeled quantitatively by varying the fraction of the incident UV-visible radiation absorbed by a particle.

Second, this process can modify the scattered and reflected light spectrum, possibly warranting some reinterpretation of the observations based solely on the albedos and "colors" appropriate for pure, unirradiated ices. Perhaps more significantly, this luminescence provides a new spectroscopic tool to probe the nature of the cometary organic refractory materials present both on the nucleus's surface as well as from the grains in the coma provided it could be detected in competition with the scattered light. In this regard, the emission between 300 and 600 nm measured from the inner coma of comet P/Halley reported by Moreels et al. (1994) is an example. In addition to the possible emission of molecules as described by Moreels et al. (1994), luminescence from the complex organic materials in the ice or present as refractory dust grains could contribute to the observed structure and underlying continuum.

4.2. Reflection from Icy Bodies

The broad emission in the visible to near-IR may also have implications for our understanding of the surface composition of planets, satellites, moons, comets, and asteroids in our and eventually in other planetary systems. The surfaces of many of these objects may once have contained considerable amounts of ices similar to the ones reported here. Nonvolatile organic residues have been included in compositional modeling of several objects in the solar system with red visual color and low albedo (e.g., Wilson & Sagan 1995; Grundy & Fink 1996; Cruikshank et al. 1998b; Owen et al. 2001). A qualitative example of how such broad emission may contribute to the measured reflectance spectrum is shown in the case of Iapetus.

It has been long known that the Saturnian satellite Iapetus exhibits an extreme dichotomy in the amount of sunlight reflected from its leading and trailing hemispheres (Cassini

1673). The dark, leading hemisphere has a geometric albedo of less than 10% while the bright, trailing hemisphere has a geometric albedo of ~50% (see Cruikshank et al. 1998a). At visual and near-IR wavelengths (~0.3–1.0 μm) the spectrum of the leading hemisphere is distinctly red with a weak and broad reflectance minimum near 0.67 μm (Vilas et al. 1996). Vilas et al. (1996) attributed this feature to charge transfer absorption of the iron oxide minerals goethite and hematite. However, Owen et al. (2001) illustrated that the reflectance spectrum of Iapetus's dark hemisphere at longer wavelengths (to 2.5 μm) was inconsistent with these minerals. Wilson & Sagan (1995) and Owen et al. (2001) used Hapke scattering models (see Hapke 1993, p. 455, and references therein) to evaluate the composition of the leading hemisphere of Iapetus. All of the models that provided a good comparison to the observational data included a nonvolatile residue component to reproduce the red coloration. Given the results of these models, we suggest that the broad feature centered near 0.6 μm might arise from luminescence of materials similar to the nonvolatile residues discussed here. Such a local maximum at 0.6 μm could impose an apparent reflectance minimum near 0.67 μm. To qualitatively illustrate this possibility we use the data of Vilas et al. (1996) because in their study the spectrum sampled significantly more of the leading hemisphere of Iapetus than the more recent data of Buratti et al. (2002).

Emission due to UV excitation is an additive effect resulting in more photons in the region of emission. We fitted a straight baseline to the data of Vilas et al. (1996) to represent the continuum color of Iapetus. To this baseline we have added the emission spectrum of the 9 month old residue (Fig. 7), multiplied by a scaling factor. The scaling factor was varied until a best fit with the Iapetus data was achieved. This synthetic spectrum is compared to the reflection spectrum of the leading side of Iapetus in Figure 9. While comparison between broad features can be forgiving of minor frequency and structural mismatches, the similar-
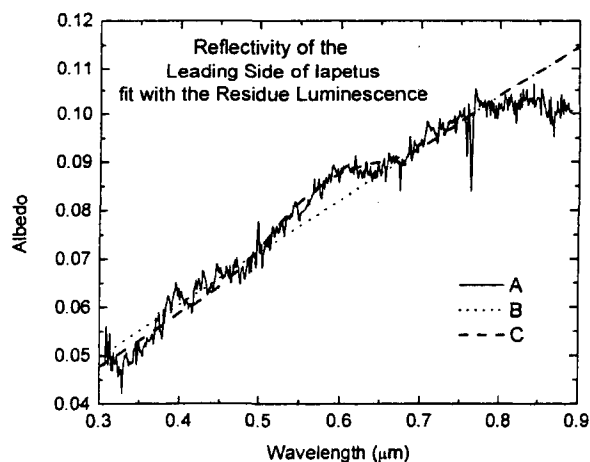

FIG. 9.—Reflection spectrum of the leading side of Iapetus (solid line, A), fitted with a straight baseline to represent the overall slope of the data (dotted line, B). The dashed line (C) shows the emission spectrum of the 9 month old residue shown in Fig. 7, multiplied with a scaling factor and added to the baseline. One can clearly see the striking resemblance between the synthetic and the observed spectra.

ities between the simulated and the measured spectra are very striking.

This simple example illustrates how the UV-pumped luminescence of surface ices and their residues could influence the spectra of solar system objects in significant ways. Furthermore, as discussed above, the emissivity of these ices and residues is temperature dependent, suggesting that luminescence should be more pronounced on colder objects. Perhaps a test of this hypothesis would be to follow an eccentric object, e.g., comet or Centaur, and monitor its reflectance spectrum as a function of heliocentric distance, correcting for the variation of UV flux with distance.

5. CONCLUDING REMARKS

The results presented here are aimed at showing, qualitatively, that cosmic ices processed with VUV light or perhaps through ion bombardment undergo reactions that result in photoluminescent chromophores, whose luminescence properties remain even after the ices are sublimed off. The next most important observation is the strong temperature dependence of the luminescence, which increases 1 order of magnitude in going from 300 to 15 K. However, there are several aspects that need to be quantified and further investigated. One of the most challenging aspects would be to quantify the quantum efficiency of the emission. Another would be to obtain a handle on the chemical composition, structural assignment, and spectroscopic properties of the molecules (neutral, radical, or ionic) generated in these ices. If achieved, these data can be used to quantitatively assign the composition of low-temperature ices and/or ice residues that are responsible for changes in optical properties, as suggested here for the case of Iapetus.

In this article we have purposefully avoided "postulating" the nature of the residue's chemical composition for the following reasons. As mentioned earlier, it is known from the mass spectroscopic studies that the residue consists of several hundreds of different molecules. Our experiments

in the past also showed that amino acids are also formed in these ices upon irradiation. Thus, given the complexity of reactions that occur during the ice irradiation and during the warm-up, any enthusiastic assignment of the luminescence to a class of species (e.g., aldehydes, acids, etc.) may be misleading. Based on the fact that the luminescence region is broad but does not change in spectral character upon warm-up or photolysis (except for efficiency), we can conclude that the chromophores do not change in their optical properties significantly. A possible explanation to account for this observation is cross-linking between the luminescent species. The presence or absence of N having no influence on the luminescence indicates that nitrogen does not affect the chromophore's optical behavior. However, this does not exclude nitrogen in the molecules. Finally, because of the fact that the luminescence increases almost 1 order of magnitude upon cooling the residue to 15 K from room temperature, we can infer that the emission is phosphorescence and the chromophores are likely to contain carbonyl groups. Carbonyl groups are known to be nonfluorescent normally but show strong phosphorescence at low temperatures. Again, caution should be exercised with this interpretation until time-resolved spectroscopic studies have been carried out to obtain lifetimes of the luminescence of the irradiated ice versus its residue.

REFERENCES

Allamandola, L. J., Sandford, S. A., & Valero, G. 1988, Icarus, 76, 225
Bernstein, M. P., Dworkin, J. P., Cooper, G. W., Sandford, S. A., & Allamandola, L. J. 2002, Nature, 416, 401
Bernstein, M. P., Sandford, S. A., Allamandola, L. J., Chang, S., & Scharberg, M. A. 1995, ApJ, 454, 327
Birks, J. B. 1970, Photophysics of Aromatic Molecules (London: Wiley)
Blake, D., Allamandola, L. J., Sandford, S. A., Hudgins, D., & Freund, F. 1991, Science, 254, 548
Buratti, B. J., Hicks, M. D., Tryka, K. A., Sittig, M. S., & Newburn, R. L. 2002, Icarus, 155, 375
Cassini, J. D. 1673, Philos. Trans. R. Soc., 8, 5178
Chillier, X. D. F., Stone, B. M., Joblin, C., Salama, F., & Allamandola, L. J. 2002, J. Chem. Phys., 116, 5725
Cottin, H., Gazeau, M. C., Benilan, Y., & Raulin, F. 2001a, ApJ, 556, 417
Cottin, H., Szopa, C., & Moore, M. H. 2001b, ApJ, 561, L139
Crifo, J. F. 1987, J. de Phys. Suppl., 48, C1-587
Cruikshank, D. P. 1997, in ASP Conf. Ser. 122, From Stardust to Planetesimals, ed. Y. J. Pendleton & A. G. G. M. Tielens (San Francisco: ASP), 315
———. 1999, in Laboratory Astrophysics and Space Research, ed. P. Ehrenfreund et al. (Dordrecht: Kluwer), 37
Cruikshank, D. P., Brown, R. H., Calvin, W. M., Roush, T. L., & Bartholomew, M. J. 1998a, in Solar System Ices, ed. B. Schmitt, C. de Bergh, & M. Festou (Dordrecht: Kluwer), 576
Cruikshank, D. P., et al. 1998b, Icarus, 135, 389
Demyk, K., et al. 2001, A&A, 368, L38
Dworkin, J. P., Deamer, D. W., Sandford, S. A., & Allamandola, L. J. 2001, Proc. Natl. Acad. Sci., 98, 815
Ehrenfreund, P., & Charnley, S. B. 2000, ARA&A, 38, 427
Gerakines, P. A., Moore, M. H., & Hudson, R. L. 2001, J. Geophys. Res., 106, 33381
Gibb, E. L., et al. 2000, ApJ, 536, 347

Greenberg, J. M., & Li, A. 1998, A&A, 332, 374
Greenberg, J. M., et al. 2000, ApJ, 531, L71
Grundy, W. M., & Fink, U. 1996, Icarus, 124, 329
Hapke, B. W. 1993, Theory of Reflectance and Emittance Spectroscopy (New York: Cambridge Univ. Press)
Hudson, R. L., & Moore, M. H. 2001, J. Geophys. Res., 106, 33275
Kobayashi, K., et al. 2001, Adv. Space Res., 27, 207
Kochi, A., & Kuroda, T. 1990, Nature, 344, 134
Langford, V. S., McKinley, A. J., & Quickenden, T. I. 2000, Accounts Chem. Res., 33, 665
McDonald, G. D., Whited, L. J., Deruiter, C., Khare, B. N., Patnaik, A., & Sagan, C. 1996, Icarus, 122, 107
Moore, M. H., Hudson, R. L., & Gerakines, P. A. 2001, Spectrochim. Acta A, 57, 843
Moreels, G., Clairemidi, J., Hermine, P., Brechignac, P., & Rousselott, P. 1994, A&A, 282, 643
Muñoz Caro, G. M., et al. 2002, Nature, 416, 403
Owen, T. C., et al. 2001, Icarus, 149, 160
Roush, T. L. 2001, J. Geophys. Res., 106, 33315
Schmitt, B., de Bergh, C., & Festou, M. 1998, Solar System Ices (Dordrecht: Kluwer)
Schutte, W. A., Allamandola, L. J., & Sandford, S. A. 1993, Science, 259, 1143
Smith, T. L., & Witt, A. N. 2002, ApJ, 565, 304
Strazzulla, G., & Palumbo, M. E. 2001, Adv. Space Res., 27, 237
van IJzendoorn, L. J. 1985, Ph.D. thesis, Leiden Univ.
Vilas, F., Larson, S. M., Stockstill, K. R., & Gaffey, M. J. 1996, Icarus, 124, 262
Wdowiak, T. J., Donn, B., Nuth, J. A., III, Chappelle, E., & Moore, M. 1989, ApJ, 336, 838
Wilson, P. D., & Sagan, C. 1995, J. Geophys. Res., 100, 7531